EMBEDDED DATA ACQUISITION PLATFORM FOR LOW SPEED AUTOMATED SURFACE MEASUREMENTS ON ASPHALT

by

JOSEPH JOEMON JOSE MULLASSERY

Presented to the Faculty of the Graduate School of

The University of Texas at Arlington in Partial Fulfillment

of the Requirements

for the Degree of

MASTER OF SCIENCE IN ELECTRICAL ENGINEERING

THE UNIVERSITY OF TEXAS AT ARLINGTON

MAY 2015

Acknowledgements

I would like to thank all people who have helped and inspired me during my master's thesis and study work. I especially want to thank my research advisor, Dr. Roger Walker, for his guidance during my research and study at University of Texas at Arlington.

His encouragement, support and enthusiasm made it smooth and easy for me in the preparation and completion of this study. In addition, he was always accessible and willing to help me as well as my colleagues with the research. As a result I was successfully able to complete my research work and write this thesis.

Last but not the least; I would like to thank my parents for their support throughout my studies and their faith which made it possible for me to reach at this level.

April 20, 2015

Abstract

EMBEDDED DATA ACQUISITION PLATFORM FOR LOW SPEED AUTOMATED SURFACE MEASUREMENTS ON ASPHALT

Joseph Mullassery Joemon Jose, MS

The University of Texas at Arlington, 2015

Supervising Professor: Roger Walker

The study is to be performed with the main goal of analyzing the existing portability and scalability problems of the existing Road profile measurement for TXDOT and improving it by making a system which is much more scalable and portable.

Along with the above, another important aspect of this research study is to develop an algorithm using a new technique based on a different type of sensor viz. 3-Axis Accelerometers and compute an estimate for the IRI (International Roughness Index) using the newly obtained data from our research and previously available IRI data from earlier research efforts.

The system would comprise of a central computing unit viz. Intel Galileo which will run an Operating System [Embedded Linux] which in turn will run the software application and device drivers needed to monitor, control and process the data available from the accelerometer. The hardware interface and design for the above is also within the scope of this research. A low speed wirelessly controlled, automated mobile unit was also designed to mount the sensor apparatus.

The main parameter we are aiming at estimating from the above exercise is the International Roughness Index which helps in the determination of the surface characteristic and thus define the profile information.

Table of Contents

List of Illustrations

List of Tables

Chapter 1

INTRODUCTION

Roadways and pavements deteriorate due to factors such as vehicle loads, impact loads and severe weather conditions.

Road damage due to natural hazards is unavoidable, it is still possible to prevent failures due to structural damage. Bridge damage caused by impact loads of trucks, overloaded vehicles, wind, rain and water which causes slow deterioration of the bridge structure can also be prevented with proper maintenance procedures.[1]

Below are some examples of roadway and bridge failures which happened due to poor maintenance and lack of inspection.

Figure 1-1 Road Damage examples due to lack of maintenance

These kinds of disasters may be avoided by periodic maintenance activities in the form of road or surface profile measurement. Road surface profiling is an important part of highway and pavement engineering. Systems exist to collect real-time continuous highway-speed measurements of longitudinal profiles of road surfaces. Using these measurements, the International Roughness Index (IRI) or Ride Number (RN) is

calculated. Both of these numbers are expressions for the roughness (and therefore ride comfort) of a road surface.[2]

Typical road profiling systems consists of non-contact laser sensors to measure to the road surface, distance encoders to measure the traversed distance and accelerometers to compensate for the effects of the vehicles movement. There are specialized road profiling systems for transverse profile, rut depth, macro texture and other shape. [2]

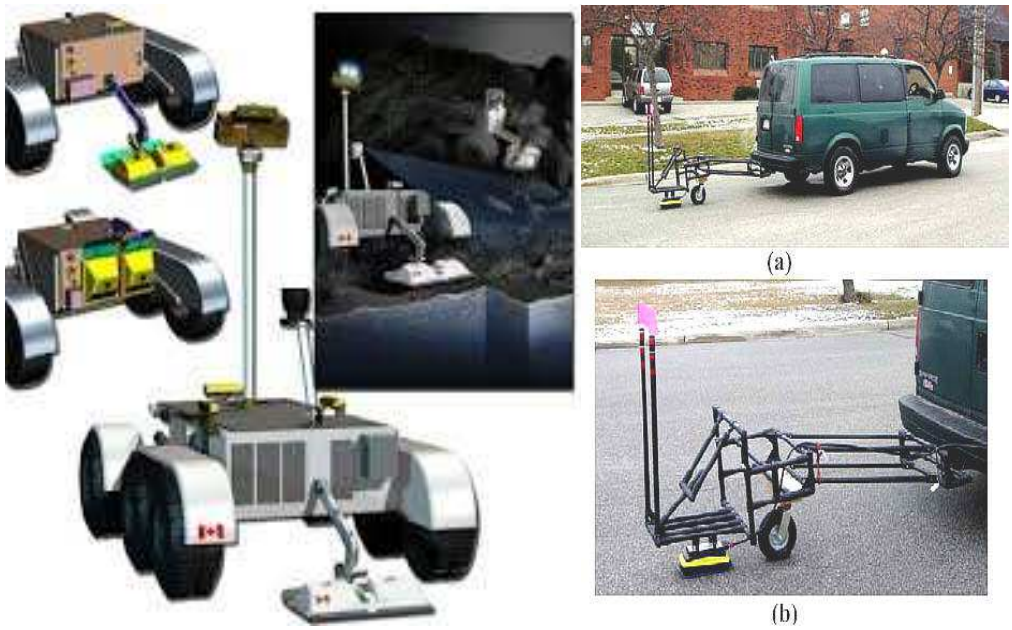

Figure 1-2 Typical Road Profiling systems[3]

Profiling is now a crucial practice for transportation departments throughout the world. Road builders, contractors and even US State DOT's (Departments of Transportation) are responsible for gathering statistical information on road surfaces including the longitudinal profile, texture information and roughness to determine coefficients of friction. [2]

1.1 Background & Problem Definition

In order to continue our discussion on IRI, it is essential to fully comprehend the necessity of IRI as well as the various techniques employed in road profile measurement systems. A profile is basically a two-dimensional slice of the road surface taken along an imaginary line. The width of the line is not a specified standard and one can measure "true profile" for any such line. [2] A profiler is an instrument which yields measurements which are correlated to the true profile of a longitudinal surface. A typical profiler combines a reference elevation, a height relevant to the reference and the longitudinal distance. [2]

Various types of devices for profile measurement can be broadly classified as

a) Rod and Level method (static).

b) Dipstick method (using inclinometers).

c) Inertial Methods (using accelerometers).

Our research focuses on the inertial method for profile measurement for several reasons. The most significant one being that empirical analysis in the past as documented in 'The Little Book of Profiling' suggests that "Accurate profile statistics can be obtained from inertial profilers". Measurements using different inertial profilers showed consistency in IRI values and a high correlation on roughness statistics thus making it more reliable. [2]

High-speed road profiling efforts began in the 60s with the GMR inertial Profilometers developed by the General Motors Research Laboratory. These profilers defined measured road profile as the summation of the mass displacement data obtained from accelerometer measurements and those obtained by laser measurements. [2]

During the 80s the South Dakota Department of Transportation (SDDOT) developed another profiling technique which was essentially using a time-based inertial

profiling algorithm. The road body displacement was sampled with respect to time and the mass acceleration was integrated with respect to time. The summation of both yielded profile data.

Measurement of profile is only half the work. The remaining half is the computation of roughness statistic. Two profile analyses that are of primary importance to researchers according to the authors of 'The Little Book of Profiling' are viz. the International Roughness Index (IRI) and the Ride Number (RN). [2] IRI has shown strong compatibility with equipment used for pavement measurement systems whereas RN is linked by statistical correlation to public opinion of ride ability. [2]

Let us take a closer look at the IRI. IRI is basically a scale of measurement of roughness based on the simulated response of a generic vehicle to the roughness in a single wheel path of the road surface[2]. It is normally reported in in/mi or m/km. Its value is measured by obtaining a reasonably accurate measurement of the profile, processing it through an algorithm that simulates the way a vehicle would respond to the roughness inputs, and accumulating the suspension travel.

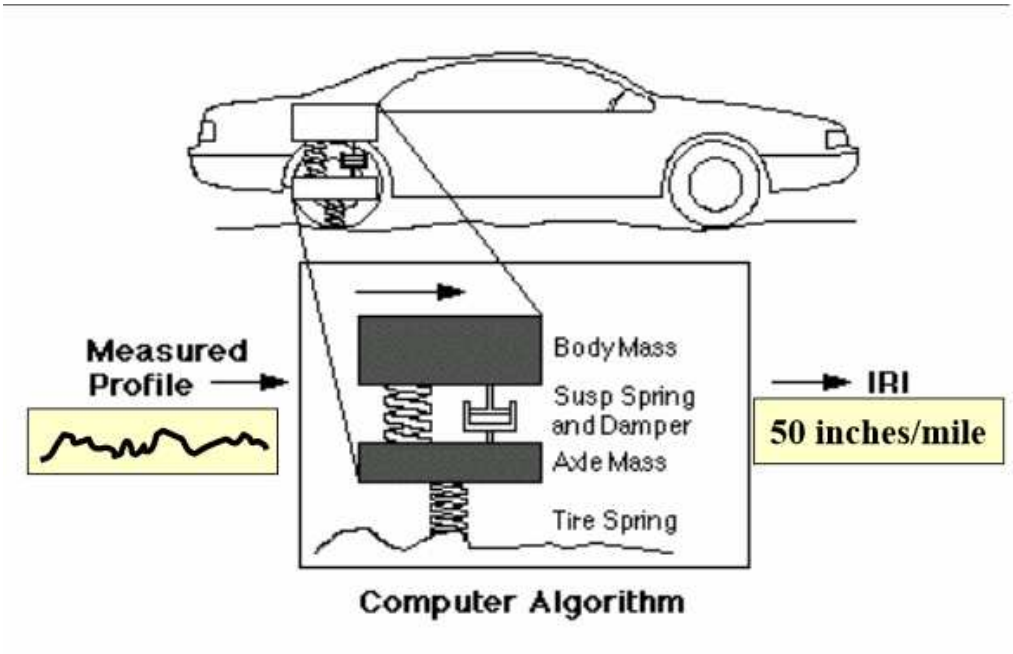

Figure 1-3 IRI Measurement Technique[4]

The IRI has the advantage of being repeatable, reproducible, and stable with time and is based on the concept of a 'golden car' whose suspension properties are known[2]. It is calculated by simulating the response of this 'golden car' to the road profile. The properties of the 'golden car' were selected in earlier research[2] to provide high correlation with the ride response of a wide range of automobiles that might be instrumented to measure a slope statistic (m/km). Researchers have found that IRI is so strongly correlated with ride quality and road loading that any other alternate statistic does not come close. The IRI, according to previous research efforts at The Minnesota Department of Transportation indicate, is time-stable, transportable, relevant and valid. [2]

Therefore, this research effort focuses entirely on the measurement and estimation of the International Roughness Index.

We will try to determine if there is a correlation between the slope variance [SV], which is computed using the acceleration measurements and the IRI of the surface which we have empirical evidence of. Using these inputs we will try to predict the IRI values for an unknown surface.

1.2 Method and approach

We are addressing two issues in this research effort. The primary issue is to find a relation between slope variance and the displacement and use that to correlate and predict the IRI values for a given surface which in our case is asphalt. The second issue is to build a portable, scalable and intelligent system which does the measurements which we will refer to as the profiling system.

The primary components of the profiling system were

a) A wirelessly controlled robot car.

b) 32-bit Intel® Quark SoC X1000 Application Processor based Intel Galileo board.

c) A sensor module mounted on the car (3-axis accelerometer ADXL345).

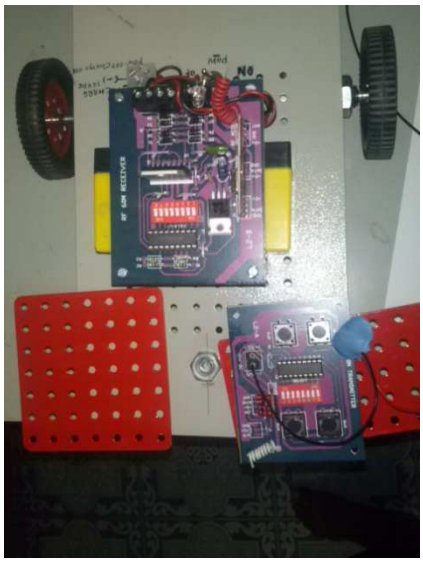

Figure 1-4 Profiling System

The basic operation of this profiling system would entail movement of the car using the remote control on the surface of which IRI has to be estimated. The sensor apparatus would be mounted firmly atop the center of the car such that there is minimum movement of the module to avoid any possible false readings. A command from the Laptop/PC to start Data Acquisition will be issued by the user which will start the data acquisition by the Galileo board mounted on the car. This will continue until stop command is issued by the user.

The data will be interpreted and processed by laptop/PC after obtaining it real-time from the car via an Ethernet cable. A basic block diagram to indicate the process is as shown below.

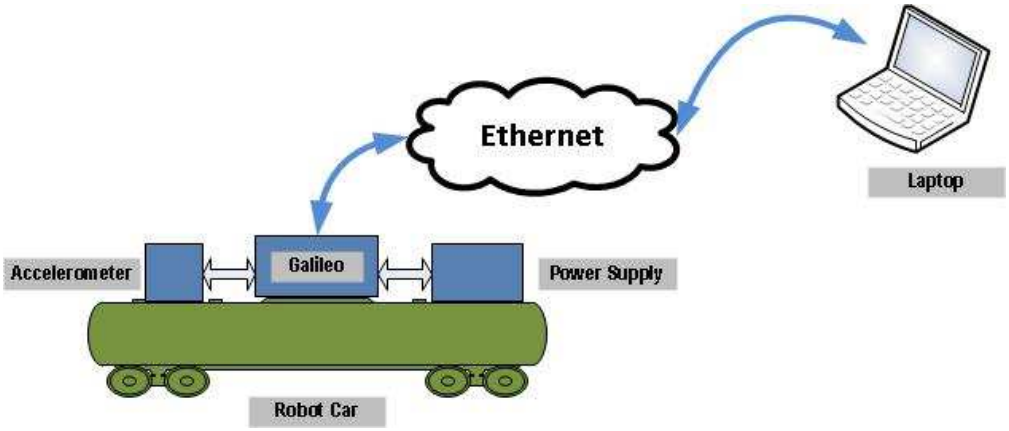

Figure 1-5 Block Diagram

Chapter 2

PLATFORM AND SENSORS

This section will describe the details of the Low speed automated Mobile unit design, construction and components followed by a brief discussion on the processor and sensors used viz. Intel Galileo board and the ADXL345 accelerometer module. This section will also discuss briefly the design issues we faced while building this profiling system and will also provide a rationale on the choice of components/devices for the profiler design.

2.1 Low Speed Automated Mobile Unit

The objective of the thesis was to be able to build our own profiling system capable of mounting the sensors and the processing unit which was revolutionary in terms of size and computation capability. Existing profiling system used across DOTs in USA are bulky and are not easily scalable or portable. Using our design and processing mechanism we would be able to reduce the size of a profiling equipment by at least a 100 times and would still be able to measure a reasonable estimate of the IRI.

Keeping this in mind, the form factor of the remote controlled mobile unit was a very important design consideration. Along with it was the load bearing capability of the system as it had to be capable to handle the combined weight of the Intel Galileo board and the ADXL 345 accelerometer module along with its own circuitry. The unit was powered by a rechargeable 12 V/1.2A Lead Acid Battery and the circuit was designed such(details is following sections) that it would be possible to operate the unit for at least 45 mins - 1 Hr without external power supply. The motors used are 5V DC 100 rpm which yield an approximate speed of 3-5 miles/hr. A metal plank of dimension 4 inches x 3 inches was clamped to the chassis of the unit to mount the ADXL345 accelerometer module. The power supply for the unit was also clamped to the chassis of the unit.

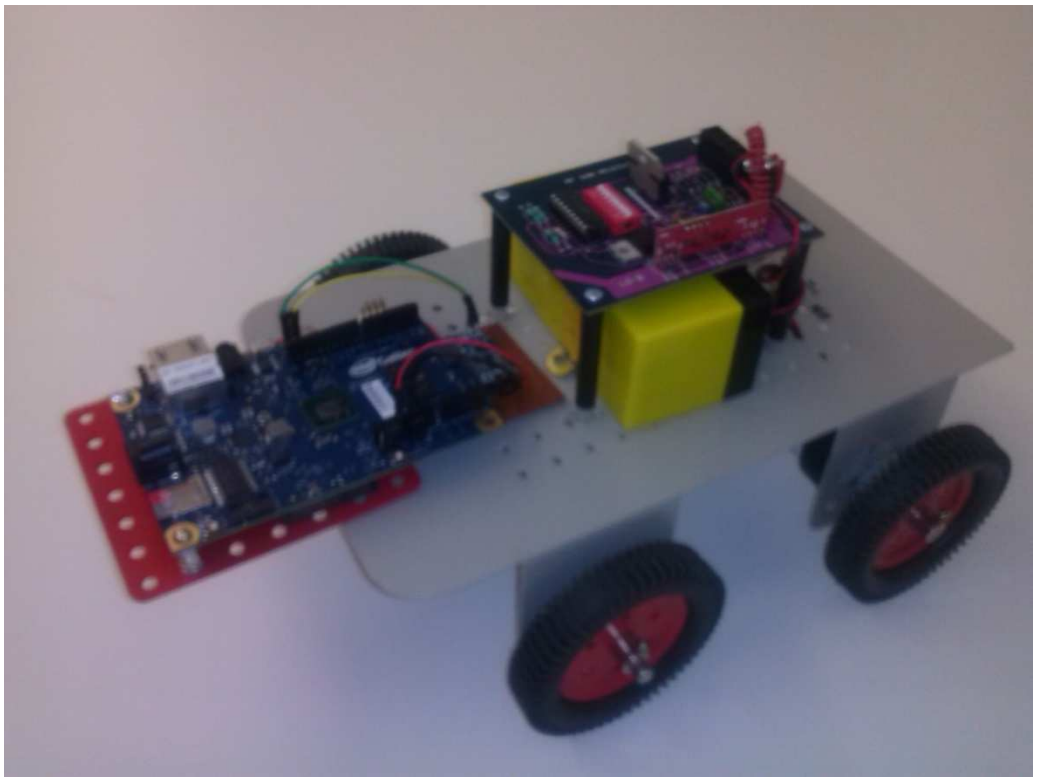

Figure 2-1 Automated Mobile Unit

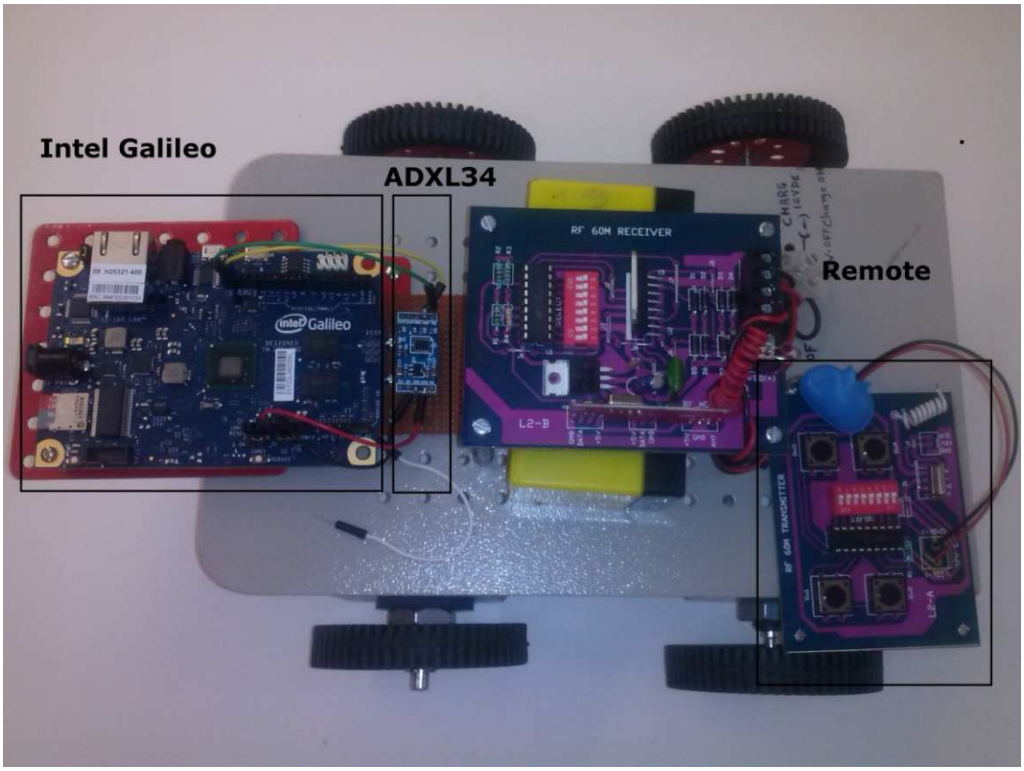

Figure 2-2 Components of the Automated Mobile Unit

2.1.1 Components and construction

The following subsection is going to focus heavily on the hardware design and is going to elaborately explain the construction of the profiling system.

2.2.1.1 Circuit Description

The circuit comprises the R.F. Transmitter & R.F. Receiver pair to transfer the coded data encoded by the integrated circuit HT-12E[5]. The transmitted data is received by the receiver circuit & decoded by the other integrated circuit HT-12D[5]. The data then decoded is passed to the integrated circuit L298N which further drives the motors in either directions[5].

The transmitter/remote control circuit comprises mainly the Data coding section and RF transmission[5]. The data coding is done by HT-12E encoding integrated circuit through the ten dip switches[5]. The forward and reverse motion of the two motors are controlled by four tactile switches. The coded data is further transmitted to the RF Module which transmits this data to the receiver[5].

The circuit comprises mainly the RF receiving & Data decoding section and Motor driving section. The R.F. is firstly received by receiver module the data so received is passed to data decoding section and is done by HT-12D decoding integrated circuit through the ten dip switches[5]. The forward and reverse motion of the two motors are controlled by the key pressed from the transmitter. The forward & reverse motion to the motor is governed by the I.C. L298N[5]. The pulses on the pin 5,7 decides the motion of the motor 1 & on pin 10,12 decides the forward and reverse motion of the motor 2[5].

Below are the list of components used in the construction of the automated mobile unit.

Table 2-1 Components List

Transmitter	
Type/Name	**Value/function**
Resistor	1M Ohm (1/4 Watt)
Diode	1N4148
Encoder	HT-12E
9V Battery Snapper	
SW1-SW4	Switches
ASK Module	RF Module (300-433 MHz)
Receiver	
Type/Name	**Value/function**
Resistors	R1,R2=1K, R3=2.2K, R4=47K
Capacitors	C1=100uF/25V, C2=0.1uF, C3=0.22uF
Decoder	HT-12D
Motor Control Drive	L298N
Linear Regulator	7805
Diodes	1N4007

2.2.1.2 Circuit Diagrams

The circuit shown below is the transmitter circuit for the remote control.

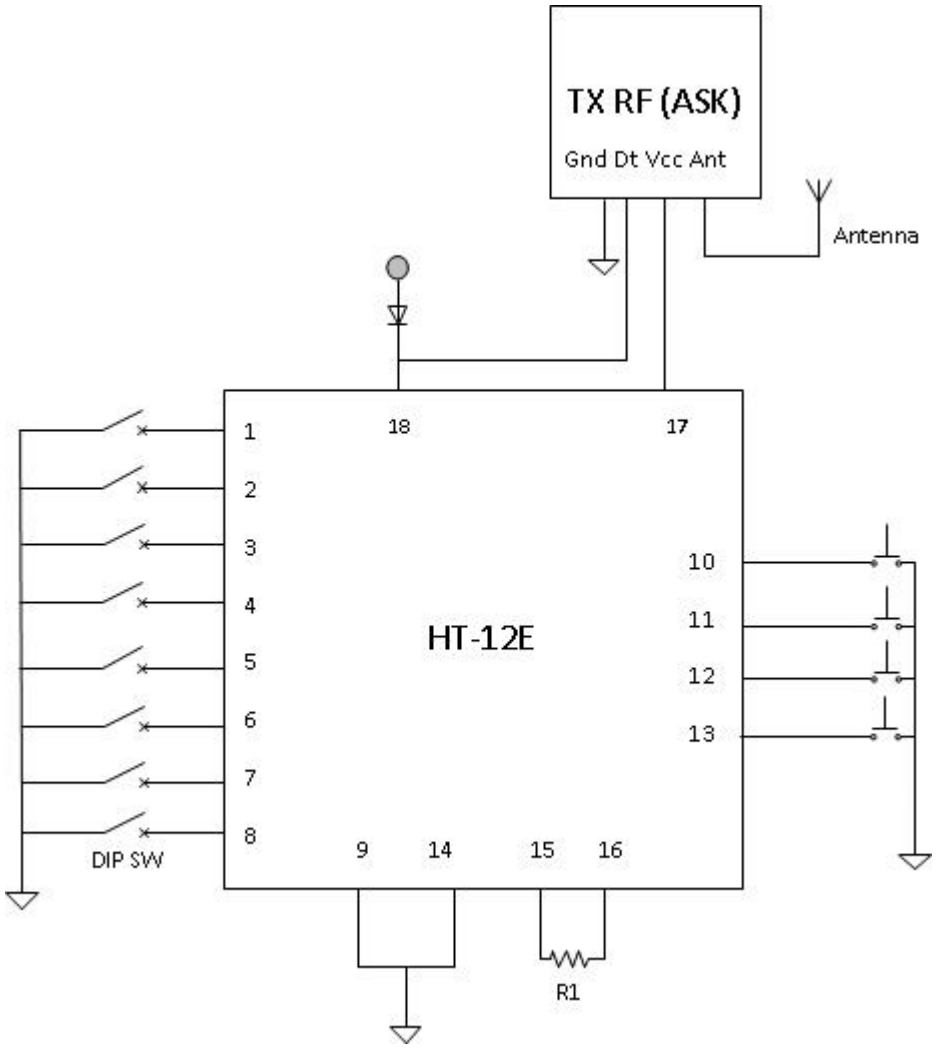

Figure 2-3 Transmitter Circuit Diagram

The circuit shown below is the Power Supply circuit for Receiver section on the Mobile Unit.

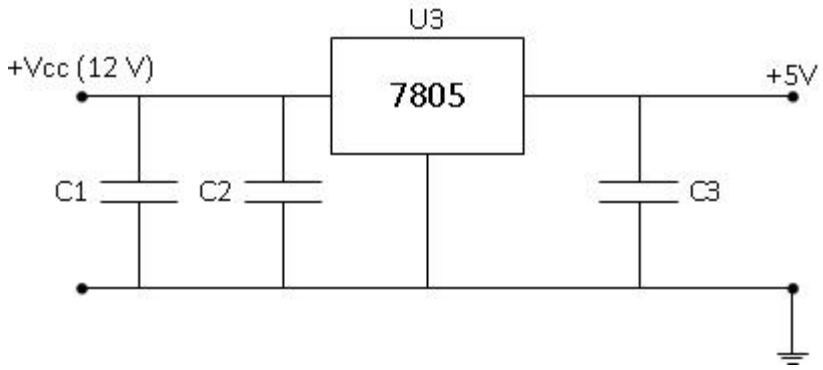

Figure 2-4 Receiver Power Supply Circuit Diagram

And finally the circuit shown below describes the RF receiver and the motor control circuitry of the Profiling System.

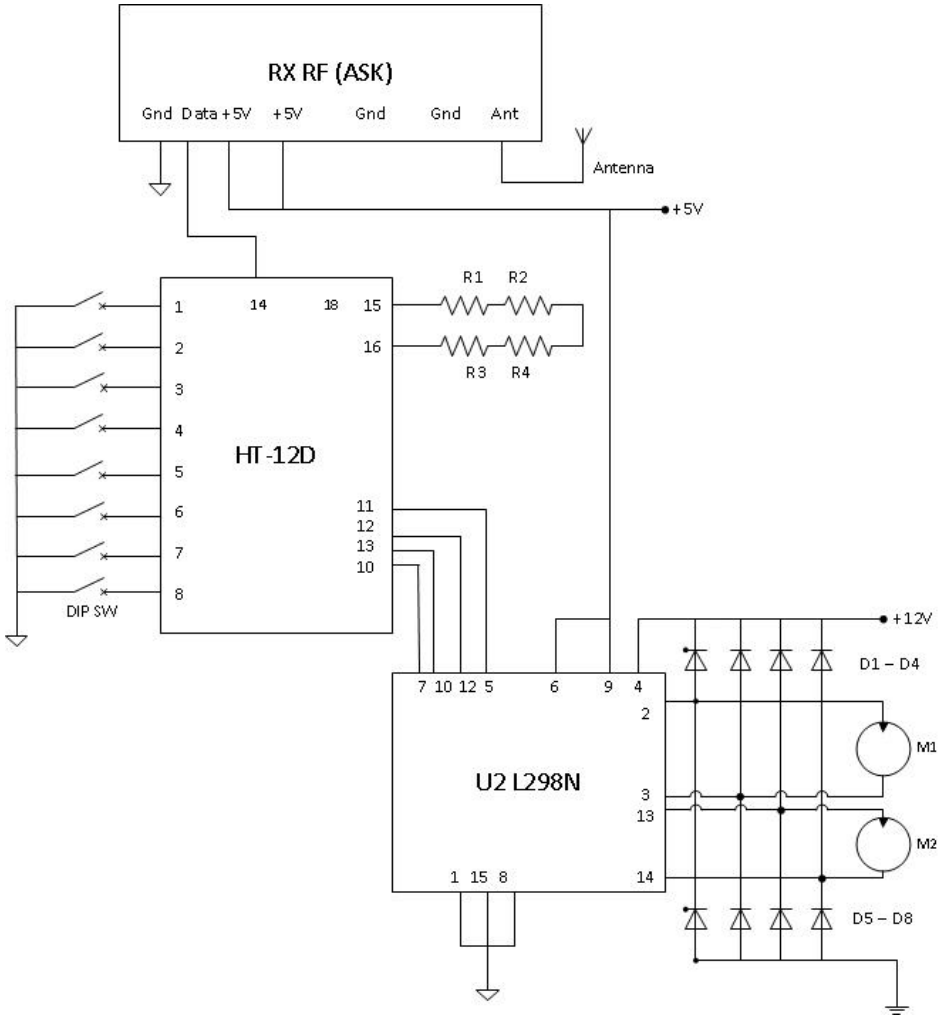

Figure 2-5 Profiling System Circuit Diagram

2.1.2 Setting up measurement apparatus

Measurement apparatus implies the Intel Galileo Board and the Accelerometer module which is mounted atop the Profiling System. It is fastened to the chassis as shown in fig 2-2.

2.2 Processing Unit and Sensor

This section focuses on the second part of the Profiling system viz. sensor and the processing unit. We will first discuss about the processing unit options that were

available during our initial estimation and requirement gathering phase and our rationale for choosing the platform which we eventually used for the system. This section will also describe in great details the features of the platform we are using and its different modes of operation and the one we used for our design. It will briefly discuss the operating system specifics for the platform as well.

The later part of this section will describe in detail the sensor used for our profiling application. We will discuss its operation, features and the role it plays in our research work.

2.2.1 Platform and Processor selection

In the initial stages of our research, there were many SBC solutions which we had considered to be the central data acquisition and processing unit which would get interfaced with the sensor. Out of all the options available, the three major contenders we had shortlisted were the Intel NUC board, BeagleBone Black and the Intel Galileo.

Intel NUC had already been proved as a reliable resource since it was being used in parallel research efforts. However, the power requirements and the form factor of NUC was beyond what we could support on a low speed, low power automated vehicle. Also, the NUC is more sophisticated and high end that what this application required. We realized that the NUC is better suited for applications which require very high processing power and can support its cost, size and power requirements.

As a result, Intel Galileo was the de facto choice for our research because of its association with the Arduino community. The Arduino community is a well known one stop solution for a wide variety of embedded products. Apart from that, they also had supporting daughter boards, lots of example software and a easy-to-use and get started interface with the Intel Galileo solution making it our choice. The counterpart,

BeagleBone Black would have a huge ramp up time as the content and support is not as organized as Arduino.

2.2.1.1 Intel Galileo Features

The Galileo is Intel's toe-dip into the Arduino waters. It features their Quark SoC X1000 processor – a relatively new, **x86-based**, low-power embedded system-on-a-chip. The 32-bit processor can run at up to 400MHz, and it has 512 KB SRAM built-in. The Galileo board supports the Quark with a wide range of external peripherals[6].

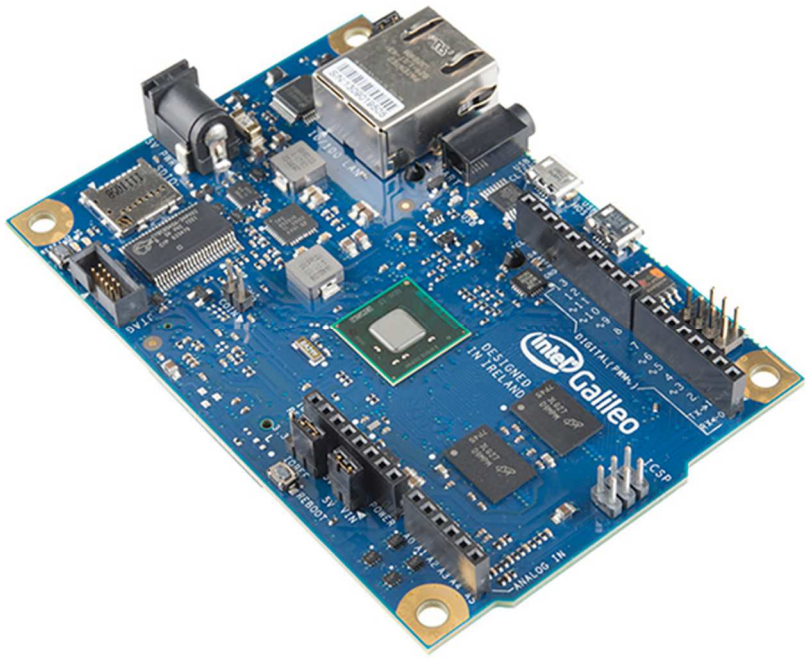

Figure 2-6 Intel Galileo

The Galileo board is also software compatible with the Arduino Software Development Environment (IDE), which makes usability and introduction a snap[6]. In addition to Arduino hardware and software compatibility, the Galileo board has several PC industry standard I/O ports and features to expand native usage and capabilities beyond the Arduino shield ecosystem[6]. A full sized mini-PCI Express slot, 100Mb

Ethernet port, Micro-SD slot, RS-232 serial port, USB Host port, USB Client port, and 8MByte NOR flash come standard on the board[6].

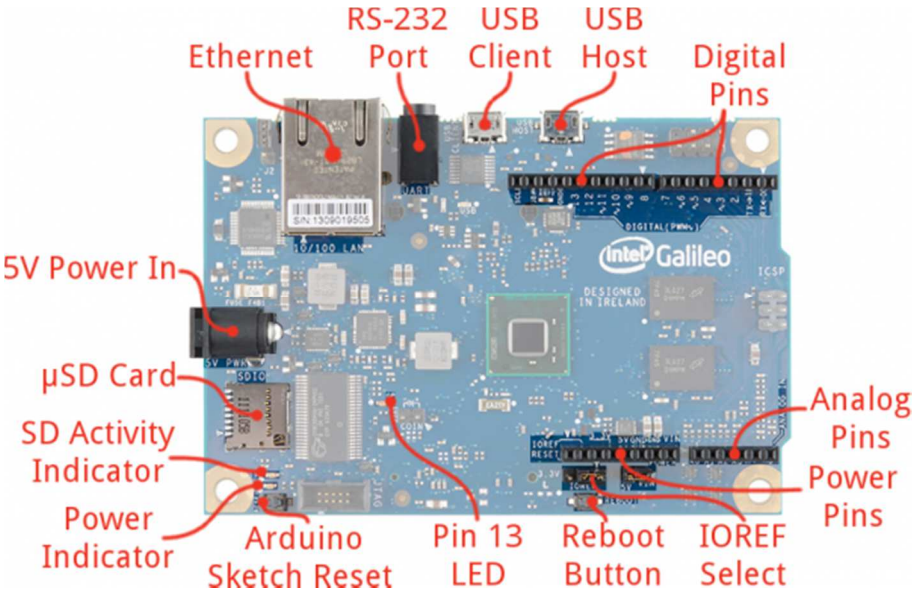

Figure 2-7 Intel Galileo Overview

Apart from the 8MB Flash (to store firmware), an 11KB EEPROM (non-volatile memory), and a µSD socket (which supports up to 32GB µSD cards) are available in the form of additional memory[6].

Galileo is powered via an AC-to-DC adapter, connected by plugging a 2.1mm center-positive plug into the board's power jack. The recommended output rating of the power adapter is 5V at up to 3Amp[6]. For the purpose of our measurements we are going to use series AA battery based power supply which provides approximately 6V/3A[6].

The following is a summary of electrical characteristics

Table 2-2 Electrical Characteristics[6]

Input Voltage (recommended)	5V
Input Voltage (limits)	5V
Digital I/O Pins	14 (of which 6 provide PWM output)
Analog Input Pins	6
Total DC Output Current on all I/O lines	80 mA
DC Current for 3.3V Pin	800 mA
DC Current for 5V Pin	800 mA

2.2.1.2 Platform Operating system information

The Intel Galileo board runs a custom Linux kernel off its flash memory on boot up. What the Galileo tries to do is meld the ease of Arduino's hardware manipulation with the power of a fully operational Linux operating system[6]. On top of it, the Arduino Development Environment gives access have access to popular **Arduino libraries** like SD, Ethernet, Wi-Fi, EEPROM, SPI, and Wire, but you can also access the Linux side of the board with **system() calls**[6].

With the on-board flash memory, the Galileo has a limited amount of space to store its Linux kernel. As such, the default Linux image is a bit gimped in terms of extra features[6]. But with an SD card, we can boot the Galileo off a bigger Linux image, which provides access to the following:

- Wi-Fi drivers
- Python
- Node.js

- SSH
- openCV
- ALSA
- V4L2

This "bigger" Linux image is obtainable from the Galileo downloads page and is copied onto an external SD card and the Intel Galileo board is made to boot from the external SD card[6].

2.2.2 Sensor Selection

The selection of the accelerometer was a fairly straightforward process because of the easy availability, low cost and excellent support available for the ADXL345 series of accelerometers.

2.2.2.1 ADXL345 features

The ADXL345 is a small, thin, low power, 3-axis accelerometer with high resolution (13-bit) measurement at up to ±16 g. Digital output data is formatted as 16-bit twos complement and is accessible through either a SPI (3- or 4-wire) or I2C digital interface[8]. The ADXL345 is well suited to measure the static acceleration of gravity in tilt-sensing applications, as well as dynamic acceleration resulting from motion or shock. Its high resolution (4 mg/LSB) enables measurement of inclination changes less than 1.0°. Several special sensing functions are provided. Activity and inactivity sensing detect the presence or lack of motion and if the acceleration on any axis exceeds a user-set level. Tap sensing detects single and double taps[8]. Free-fall sensing detects if the device is falling. These functions can be mapped to one of two interrupt output pins. An integrated, patent pending 32-level first in, first out (FIFO) buffer can be used to store data to minimize host processor intervention. Low power modes enable intelligent motion-based

power management with threshold sensing and active acceleration measurement at extremely low power dissipation[8].

The lower range (+-2G) gives more resolution for slow movements, the higher range(+-16G) is good for high speed tracking[8]. The ADXL345 is the latest and greatest from Analog Devices, known for their exceptional quality MEMS devices. The VCC takes up to 5V in and regulates it to 3.3V with an output pin[8].

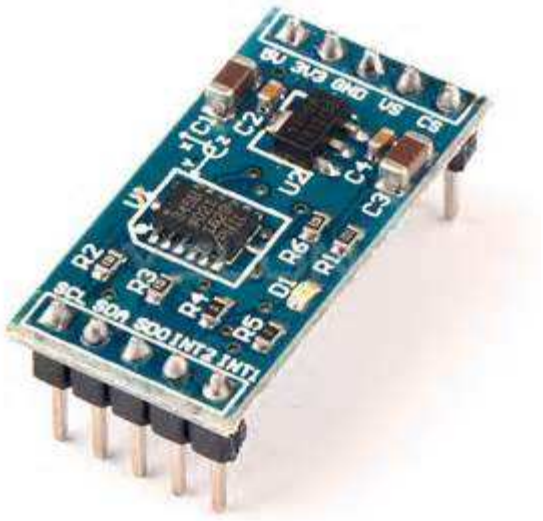

Figure 2-8 ADXL345 Overview[7]

SPECIFICATIONS

T_A = 25°C, V_S = 2.5 V, $V_{DD I/O}$ = 1.8 V, acceleration = 0 g, C_S = 10 µF tantalum, $C_{I/O}$ = 0.1 µF, output data rate (ODR) = 800 Hz, unless otherwise noted. All minimum and maximum specifications are guaranteed. Typical specifications are not guaranteed.

Table 1.

Parameter	Test Conditions	Min	Typ[1]	Max	Unit
SENSOR INPUT	Each axis				
Measurement Range	User selectable		±2, ±4, ±8, ±16		g
Nonlinearity	Percentage of full scale		±0.5		%
Inter-Axis Alignment Error			±0.1		Degrees
Cross-Axis Sensitivity[2]			±1		%
OUTPUT RESOLUTION	Each axis				
All g Ranges	10-bit resolution		10		Bits
±2 g Range	Full resolution		10		Bits
±4 g Range	Full resolution		11		Bits
±8 g Range	Full resolution		12		Bits
±16 g Range	Full resolution		13		Bits
SENSITIVITY	Each axis				
Sensitivity at X_{OUT}, Y_{OUT}, Z_{OUT}	All g-ranges, full resolution	230	256	282	LSB/g
	±2 g, 10-bit resolution	230	256	282	LSB/g
	±4 g, 10-bit resolution	115	128	141	LSB/g
	±8 g, 10-bit resolution	57	64	71	LSB/g
	±16 g, 10-bit resolution	29	32	35	LSB/g
Sensitivity Deviation from Ideal	All g-ranges		±1.0		%
Scale Factor at X_{OUT}, Y_{OUT}, Z_{OUT}	All g-ranges, full resolution	3.5	3.9	4.3	mg/LSB
	±2 g, 10-bit resolution	3.5	3.9	4.3	mg/LSB
	±4 g, 10-bit resolution	7.1	7.8	8.7	mg/LSB
	±8 g, 10-bit resolution	14.1	15.6	17.5	mg/LSB
	±16 g, 10-bit resolution	28.6	31.2	34.5	mg/LSB
Sensitivity Change Due to Temperature			±0.01		%/°C
0 g OFFSET	Each axis				
0 g Output for X_{OUT}, Y_{OUT}		−150	0	+150	mg
0 g Output for Z_{OUT}		−250	0	+250	mg
0 g Output Deviation from Ideal, X_{OUT}, Y_{OUT}			±35		mg
0 g Output Deviation from Ideal, Z_{OUT}			±40		mg
0 g Offset vs. Temperature for X-, Y-Axes			±0.4		mg/°C
0 g Offset vs. Temperature for Z-Axis			±1.2		mg/°C
NOISE					
X-, Y-Axes	ODR = 100 Hz for ±2 g, 10-bit resolution or all g-ranges, full resolution		0.75		LSB rms
Z-Axis	ODR = 100 Hz for ±2 g, 10-bit resolution or all g-ranges, full resolution		1.1		LSB rms
OUTPUT DATA RATE AND BANDWIDTH	User selectable				
Output Data Rate (ODR)[3, 4, 5]		0.1		3200	Hz
SELF-TEST[6]					
Output Change in X-Axis		0.20		2.10	g
Output Change in Y-Axis		−2.10		−0.20	g
Output Change in Z-Axis		0.30		3.40	g
POWER SUPPLY					
Operating Voltage Range (V_S)		2.0	2.5	3.6	V
Interface Voltage Range ($V_{DD I/O}$)		1.7	1.8	V_S	V
Supply Current	ODR ≥ 100 Hz		140		µA
	ODR < 10 Hz		30		µA
Standby Mode Leakage Current			0.1		µA
Turn-On and Wake-Up Time[7]	ODR = 3200 Hz		1.4		ms

Figure 2-9 ADXL345 Datasheet and Features

The following table illustrates the connection details between the Intel Galileo Board and the ADXL345 Accelerometer module.

Table 2-3 Pin Connections[8]

Intel Galileo Pins	**ADXL345 pins**
10	CS
4	SDA
NC	SDO
5	SCL
3.3V Pin	Vcc
Ground	Ground

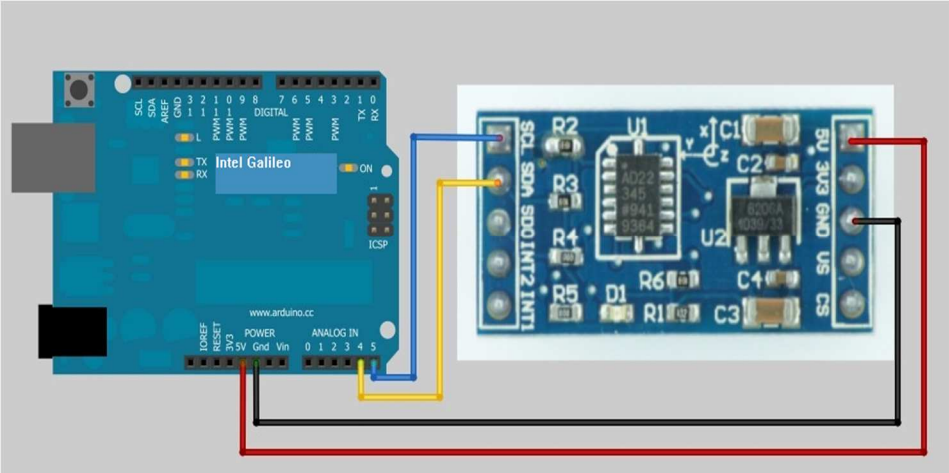

Figure 2-10 ADXL345 Pin Connection[7]

Chapter 3

MEASUREMENT AND IRI ESTIMATION

This section explains in detail the data acquisition software and the data processing mechanism to obtain the variance of the velocity data which in turn is derived from the accelerometer readings and the distance traversed. It will also explain the software initialization and setup process of the various Intel Galileo peripherals and buses which are used to communicate with the sensor(Accelerometer) and those which communicate with the Laptop/PC. The next item which will be discussed in detail is the software flow to both obtain the accelerometer reading and the slope variance from it.

This section will also focus on the method used to obtain the numerical integral of the accelerometer readings to obtain the velocity values. We will employ the trapezoidal rule for integration. A key thing to be noted here is to convert the acceleration values to appropriate values of 'G' force and in units of inches/m^2.

In the later sections, we will try to analyze the correlation between the slope variance of the velocity values and the IRI for that set. These values are calculated from a data set of road profile readings obtained previously by measuring the slope and then the variance. This data set is being considered for all the analyses in this research effort since the validity, authenticity and accuracy of this particular set has been proven beyond doubt by previous researchers working on IRI. We will discuss this in much detail in the following sections.

3.1 Data Acquisition Algorithm Details

The following figure illustrates the state diagram for the data acquisition software. Each transition has been clearly outlined and the details of each state will be explained in the due course.

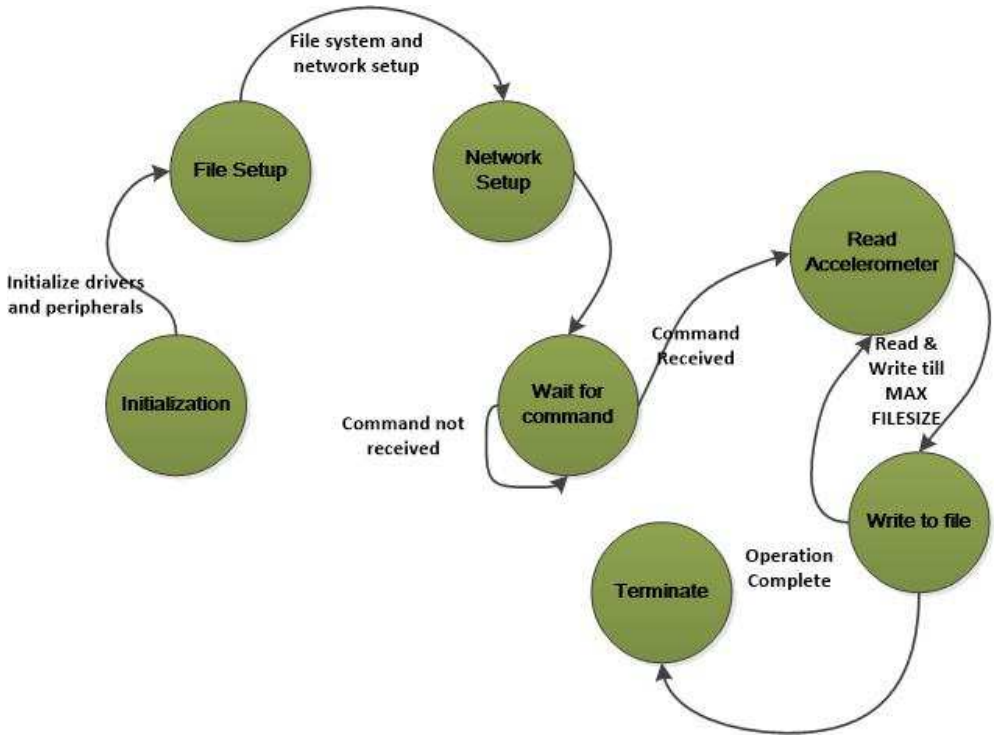

Figure 3-1 State Diagram

Before exploring the state diagram it is essential to shed some light on the operation of the platform itself. The stock on-board Linux image is lightweight and therefore does not have full operational capability or features. This can be obviated by means of booting the Galileo off an SD Card which carries the "bigger" kernel image. This allows access to several features explained earlier in this document. This also allows Arduino sketches to be persistent on system reboots.

The flow of the state diagram is as follows.

- Initialization - The various peripherals and device drivers needed for further use are initialized and setup. Variables are declared and allocated memory depending on the purpose. The drivers used specifically are the I2C, Accelerometer and Timer.

- File Setup - Raw accelerometer data is stored in a file which is later retrieved via the Ethernet to laptop/PC. This state initializes the file handles and memory allocation logic to ensure that data is not overwritten onto the file.
- Network Setup- In order to retrieve the accelerometer readings from the file, as mentioned above, an Ethernet IP address has to be allocated to this system. This is achieved by using Linux system calls to set IP address.
- Wait for command - In this state a TCP socket is opened and the program keeps waiting for a read command from the laptop/PC in a client-server fashion.
- Read Accelerometer - In this section the accelerometer data is read every 100 ms. The data is converted to an ASCII value to be stored in the aforementioned file which in this case is a text file. This operation continues until file limit is reached or user specified MAX SAMPLE VALUES have reached.
- Write to file - The ASCII data is written to the file and the program evaluates for any terminating condition to occur in the form of maximum specified samples.
- Terminate - The file is closed and the allocated memory is freed up and the program exits gracefully.

The following flowchart explains the code flow and the above state information in a little more detail.

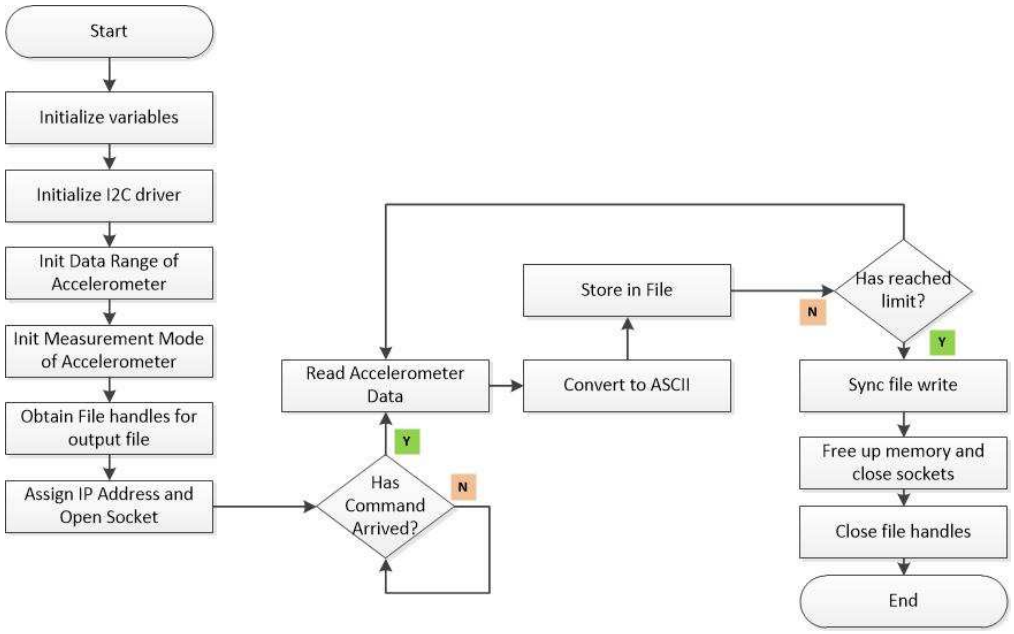

Figure 3-2 Data Acquisition Flowchart

3.2 Data Processing Details

As explained earlier the data is acquired and logged into a file which is then read by a PC application via Ethernet. The raw data has to be processed before it can be used to deliver an estimate of the IRI. Based on empirical data, my advisors guidance and statistical evidence from previous research efforts we decided to use Slope Variance of velocity.

In order to do that velocity must be computed from the integration of the plotted Acceleration curve. The technique used here is the Trapezoidal Rule for integration. The figure below illustrates the Trapezoidal Rule for numerical approximation.

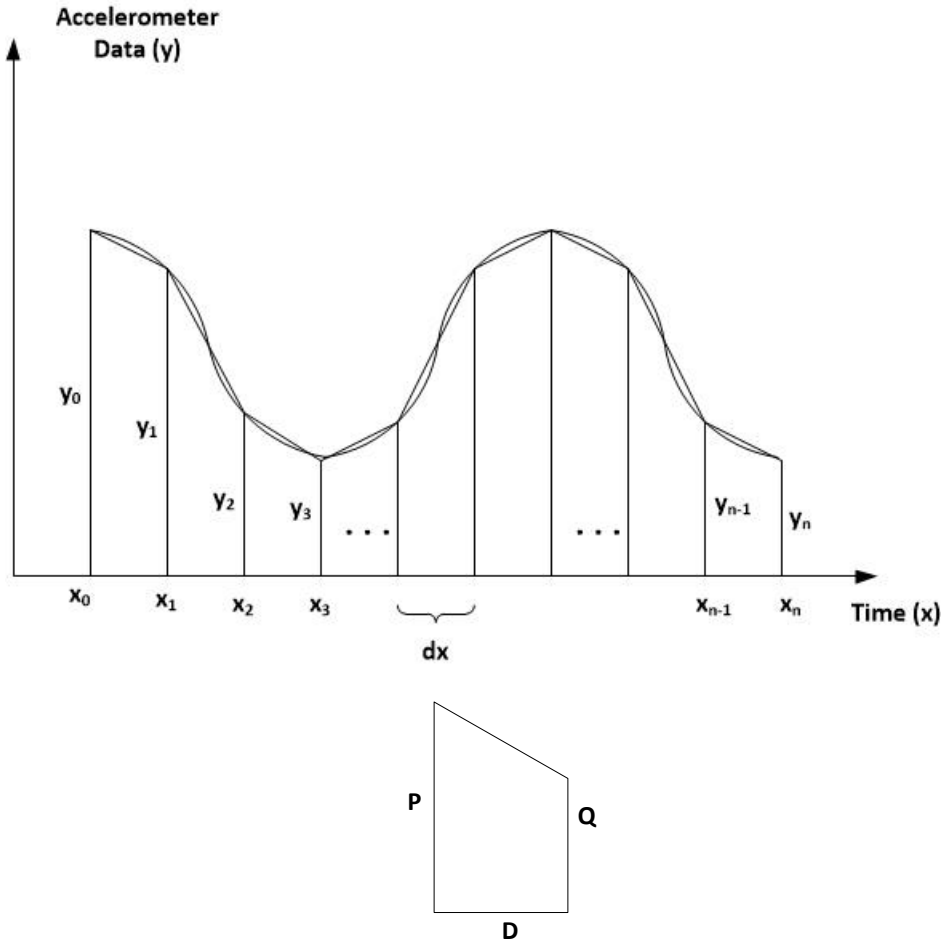

Figure 3-3 Trapezoidal Rule

The trapezoidal rule works by approximating the region under the graph of the function f(x) as a trapezoid and calculating its area. Using that the area of one trapezoid is given by

$$A = \left(\frac{P + Q}{2}\right) \times D$$

So the approximate area under the curve is found by adding the area under each of these individual trapezoids.

$$A = \frac{1}{2}(y_0 + y_1) \times dx + \frac{1}{2}(y_1 + y_2) \times dx + \cdots$$

In the above case we are measuring the acceleration values every 100 ms therefore an instantaneous area under the curve given by [$\frac{1}{2}(y_{n-1} + y_n) \times dx$] represents the velocity value per 100 ms. During analysis, care is taken to do all calculations in inches as the measured value of IRI is in *inches/mile*. We have chosen to work with *inches/mile* as the standard unit for IRI in this research endeavor for ease of analysis.

Naturally to obtain the velocity value in inches/sec, the instantaneous values have to be summed for 10 intervals of 100 ms each. Before any of this conversion it is essential to convert the raw accelerometer data into corresponding G values in *inches/s²*. The ADXL345 is setup to measure 10-bits for a $\pm$2G range. The scale is found by dividing the total range by the maximum number that can be represented by 10 bits.

$$Scale = \frac{2^2}{1024} = 0.00390625\ mG/LSB$$

In essence, this scaled accelerometer reading is converted to velocity using the Trapezoidal Rule. The variance of these velocity data points is then calculated using the formula

$$s^2 = \frac{\sum(x - x_{mean})^2}{n - 1}$$

This variance data is then used for estimation of the IRI value for that particular surface. We will discuss the IRI estimation model in the next section and derive the equation for the same.

3.3 IRI Estimation Technique

During the course of this research we were looking at a number of factors from existing road profile measurement which would result in a reasonable correlation with the IRI. We have discussed in ample detail at the beginning about the importance of IRI measurement in the field of road maintenance and construction. The primary motivation

for this effort was to be able to estimate IRI using only the accelerometer thus starting a new paradigm in the field of road profile measurement.

From previous research endeavors we were having the road profile data computed by TXDOT on US highway 77. From this road profile data we were able to extract a high correlation between slope variance on the velocity and the IRI values for those set of velocities.

Below is the road profile data obtained from the test run on US highway 77. This data was obtained by feeding the profile reading to ProVAL. ProVAL (Profile Viewing and AnaLysis) is an engineering software application that allows users to view and analyze pavement profiles in many different ways. It is easy to use and yet powerful to perform many kinds of profile analyses. ProVAL is a product sponsored by the US Department of Transportation, Federal Highway Administration (FHWA) and the Long Term Pavement Performance Program (LTPP). These ride statistics are at intervals of 528 ft.

Table 3-1 Properties of Road Profile

ID	Name	Value
258	Section Title	US77WACOK1
259	Profiling Instrument Identification	RSP_5051_Mark_III
261	Date Data Was Collected (YYYYMMDD)	20040714
262	Time Data Was Collected (HHMMSS)	******
265	Original Filename	US77WACOK1.pro
272	Agency District Number	9
274	County Number	161
281	Roadway Designation	US0077
282	Lane Identification	K1
284	Reference Marker or Milepost of Beginning Point	0382 -02.663
295	Date Last Modified (YYYYMMDD)	20150327
296	Time File Last Modified (HHMMSS)	193830
297	Date Imported (YYYYMMDD)	20150327

Table 3-2 IRI information

Interval (ft)	IRI left in/mi	IRI right in/mi
0 to 528	55.5	51.6
528 to 1,056	56.9	53.7
1,056 to 1,584	57.1	51
1,584 to 2,112	41.6	40.4
2,112 to 2,640	55.4	51.2
2,640 to 3,168	56.7	50.7
3,168 to 3,696	56.5	50.9
3,696 to 4,224	58	50.2
4,224 to 4,752	50.8	50.7
4,752 to 5,280	43.1	42.3
5,280 to 5,808	44.1	46.8
5,808 to 6,336	39.9	33.9
6,336 to 6,864	63	39.8
6,864 to 7,392	49.2	39.8
7,392 to 7,920	66.1	63.9
7,920 to 8,448	54.1	52.8
8,448 to 8,976	124.8	131.1
8,976 to 9,504	117.9	119.1
9,504 to 10,032	52	38.5
10,032 to 10,560	50.8	45.5
10,560 to 11,088	43.3	38.9
11,088 to 11,616	39.8	46.2
11,616 to 12,144	47.7	47.7
12,144 to 12,672	50.4	43.9
12,672 to 13,200	68.5	53.9
13,200 to 13,728	66.3	54.3
13,728 to 14,256	55.2	47.1
14,256 to 14,784	54.7	60.2
14,784 to 15,312	41.3	34.7
15,312 to 15,578	44.3	38.5

From Table 3-1 and Table 3-2, which were generated from ProVAL we can infer that the above data is the road profile measurement test run conducted by TXDOT in the summer of 2004.

Using above data to compute the slope and then the slope variance and we plotted it against the IRI. Below curves indicate the characteristics when slope variance of velocity for each set of 528 feet of data was mapped against the IRI in Table 3-2.

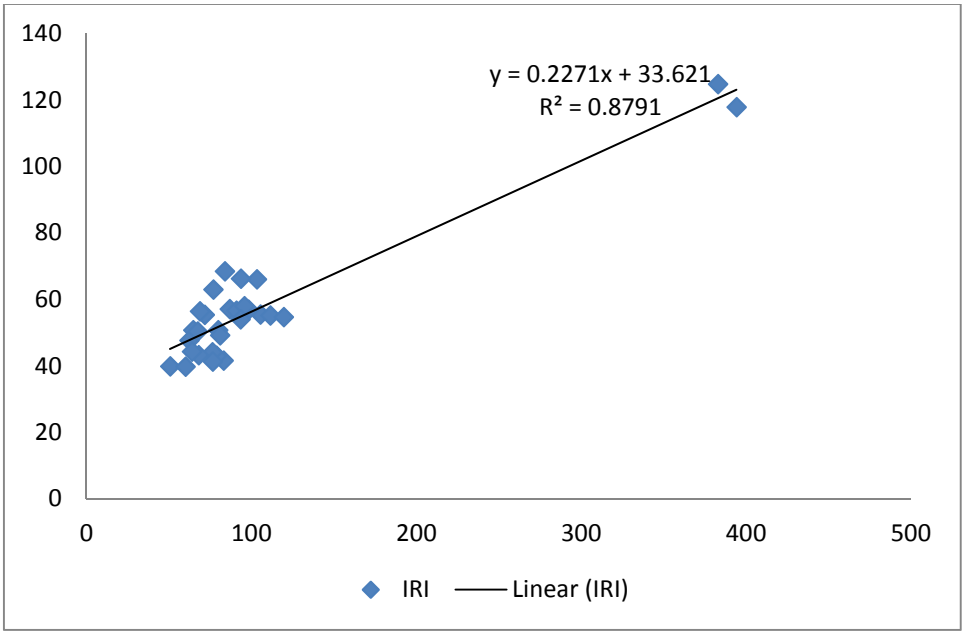

Figure 3-4 Plot for Left Profile

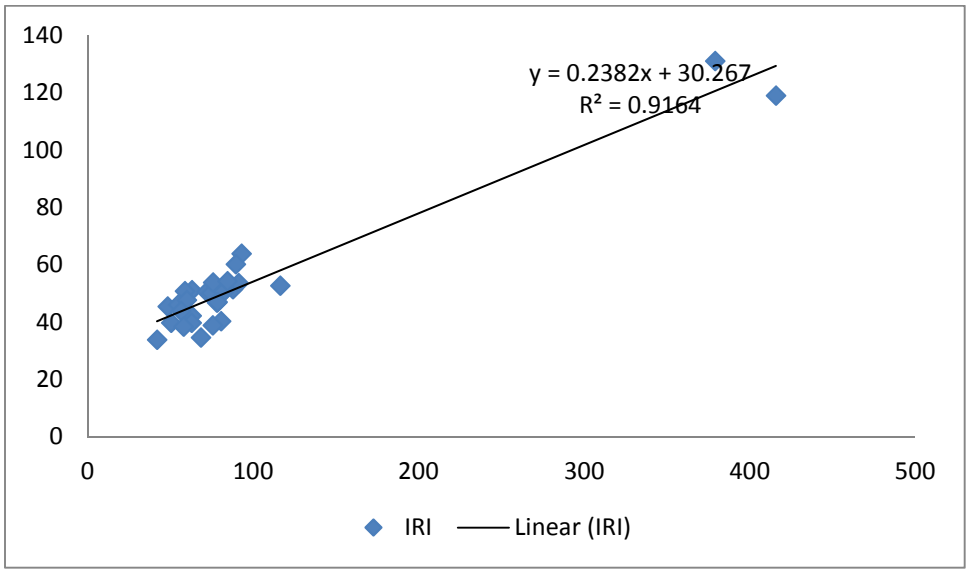

Figure 3-5 Plot for Right Profile

The above curves clearly indicate a very high correlation between the slope variance of the velocity obtained from road profile data and the IRI values. Thus we deduced that it would be possible to use the above characteristic and predict an IRI value for an unknown surface. We will cover in the next chapter the exact details of the IRI predictions done for sample runs within the UT Arlington campus.

The above analysis yields 2 equations which determine the relationship between the IRI values and the data variance viz.

$y = 0.2271x + 33.621$ with $R^2 = 0.8791$ and

$y = 0.2382x + 30.367$ with $R^2 = 0.9164$

where y - IRI values and x - slope variance of velocity

We are going to define a constant k_{IRI} or the **Walker Constant** which is going to be the predictor of IRI. In principle the constant values $\varepsilon = 33.621 \ \& \ 30.367$ are profile independent but we will consider those in the prediction of IRI. For the sake of this research we are choosing the k_{IRI} for the best fitting curve i.e. one with the highest R^2 value. For all our estimations and IRI predictions henceforth we choose $k_{IRI} = 0.2382$.

In the next chapter we will use the above constant to predict IRI values for surfaces for which we do not have IRI data readily available. The means for validating the prediction is previously available empirically obtained IRI readings for surface of the similar kind. The surface characteristic of asphalt roads varies with temperature, wear and tear, materials used, construction quality, weather and a lot of other features. In spite of these factors previous researchers in this have broadly classified types of roads and have obtained IRI values for each category of road. A drawback we faced here is the fact that the effort involved just to get TXDOT to measure profile for a small patch of road is beyond the scope and timeline of this research effort. Hence, the experience of previous researchers and the judgment and input of our thesis guide, his experience and

knowledge of various IRI values for various road types, is the yardstick we use to validate the predicted IRI using k_{IRI}.

Chapter 4

FIELD TESTING AND ANALYSIS

Before analyzing the test results it is essential to reiterate the importance of this profiling technique especially on asphalt roads. Although this method can be used on concrete, asphalt and other kinds of roads with reasonable accuracy as shown from the results below, it finds its true importance on newly laid asphalt roads. On newly laid asphalt roads, owing to its lightweight structure and automated nature, a road contractor can easily use our technique to measure instantaneous road profile. The alternative he has is to wait for the road to dry up and then get the entire profiling equipment from some state profiling authority.

In this chapter we will stress on the prediction of IRI values for different surfaces in the UT Arlington campus using the Walker constant or k_{IRI}. In order to compute the IRI, the technique used is to find the slope variance of the velocity every 50ft. The reason we use 50 ft is because to obtain the IRI information from the US77 reference data set, we use 50 ft intervals for every 528 ft of data to get the statistics.

Thus to maintain one-to-one correspondence and consistency of correlation we take slope variance at 50 ft intervals of the surface under test. In order to test our system we took measurements on two different types of surfaces and obtained predicted IRI values. One surface was a rough corridor Outside left gate of ERB and the second was partial asphalt surface on the Tri C parking lot just opposite University center. Both of these surfaces provided sufficient variety in their characteristics to be able to run our system on them and obtain values which could be compared and categorized. The details of the measurements, predictions and the nature of these surfaces is in the sections below.

4.1 Hallway/Corridor Surface(Test Run 1)

We attempted predicting the IRI value of the Corridor surface(concrete) using the Walker constant we derived in Chapter 3. The figures below illustrate the nature of the surface. We moved from a relatively smoother surface to a more rougher area. Our conclusions from the predictions also corroborated that fact. We got low IRI values for smoother patches and higher IRI values for rougher patches.

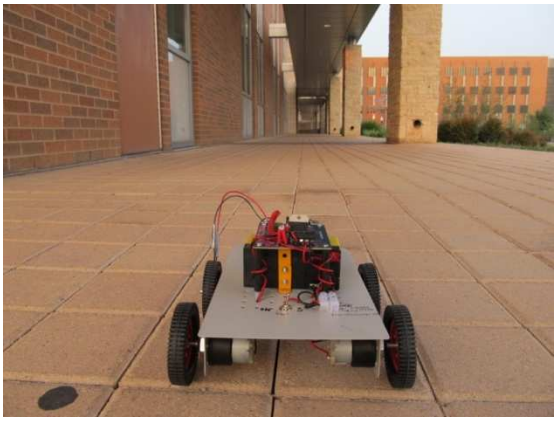

Figure 4-1 Test Run 1 - Relatively Smoother surface

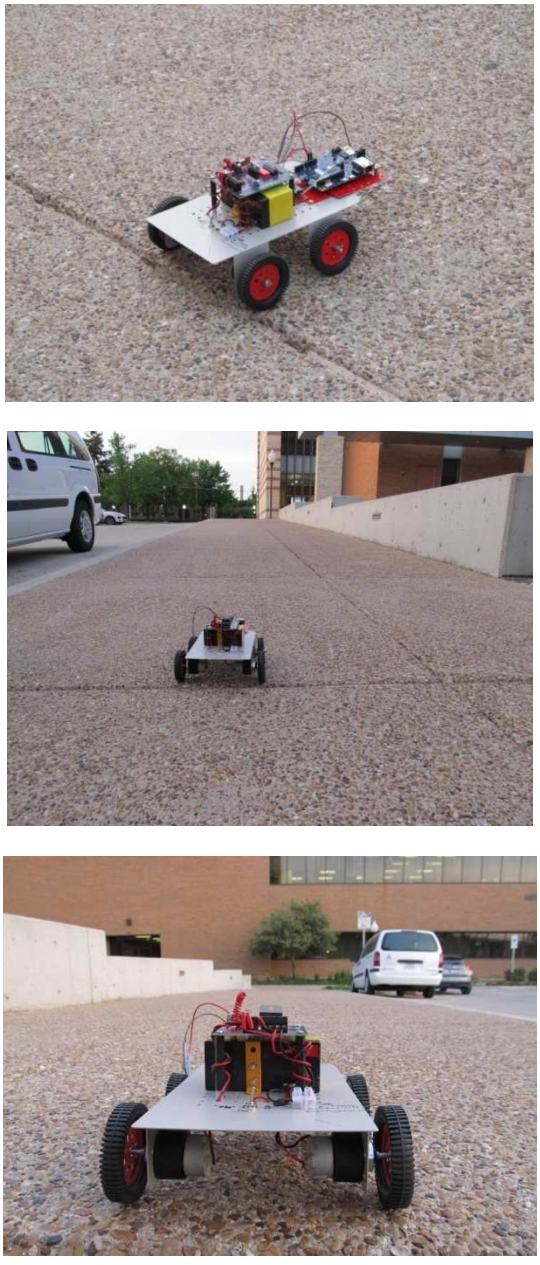

Figure 4-2 Test Run 1 - Relatively Rough surface

The figure below illustrates the trend of the velocity slope variance values across the surface.

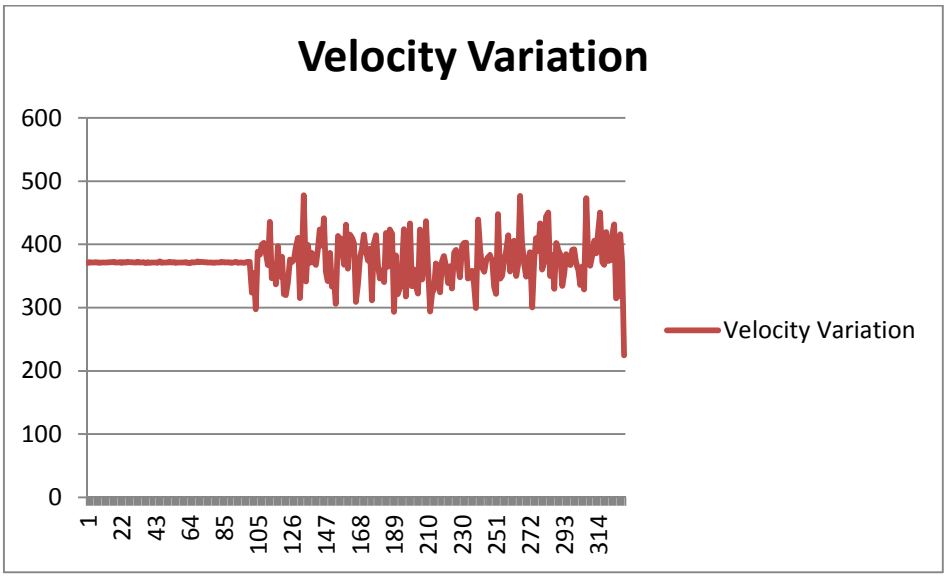

Figure 4-3 Test Run 1 - Velocity Variation with respect to distance

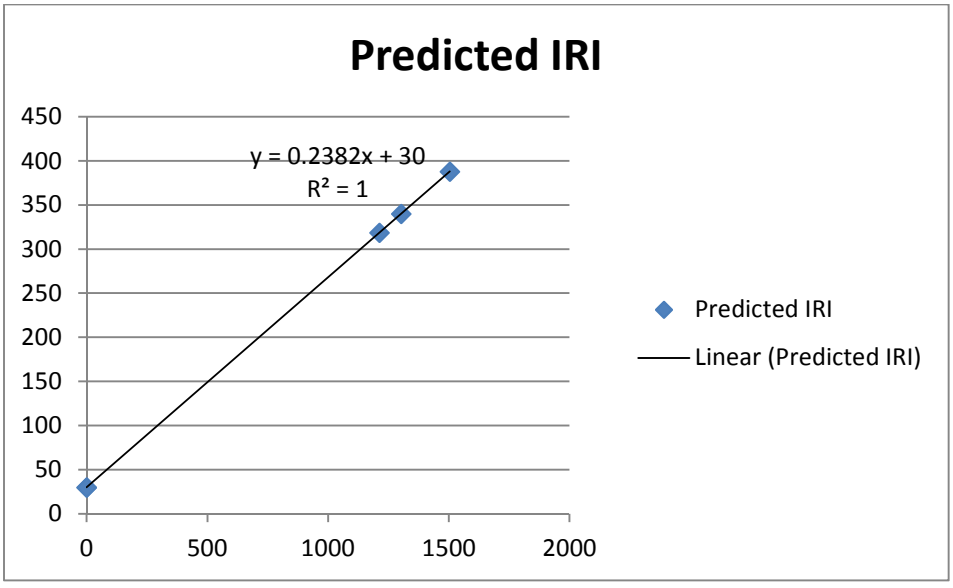

Figure 4-4 Test Run 1 - Predicted IRI

Table 4-1 Predicted IRI for Test Run-1

Distance	Velocity Variance Per 50 Ft	Predicted IRI(in/mi)	Total Variance	Total IRI(in/mi)
50	0.219735953	30.0523411	**1030.731659**	**245.5203**
100	0.198797263	30.04735351		
150	1302.382223	340.2274455		
200	1503.577768	388.1522243		
250	1211.950057	318.6865036		
300	1365.689551	355.3072511		

These IRI values were predicted using the equation $y = 0.2382x + 30.367$ with a Walker constant $k_{IRI} = 0.2382$ and constant $\varepsilon = 30.367$.

As we can observe that we get low IRI prediction indicating smoother surface for the first 100 ft equivalent of data. That information matches with Figure 4-1. For the next ~220 ft of the surface we get high IRI predictions as is clear from Figure 4-2. This data was matched, bonafied and verified by our research advisor who has been a pioneer in the field of road profile measurement for over 40 years.

4.2 Parking Lot Surface (Test Run 2)

For our next test run we tried measuring the IRI for an asphalt surface followed by the surface of a regular parking lot inside the campus. Once again we used the Walker constant for these predictions. The figures below clearly outline the nature of the surface. Once again we moved from a smoother surface to a rougher one and our predicted IRI values showed the same trend.

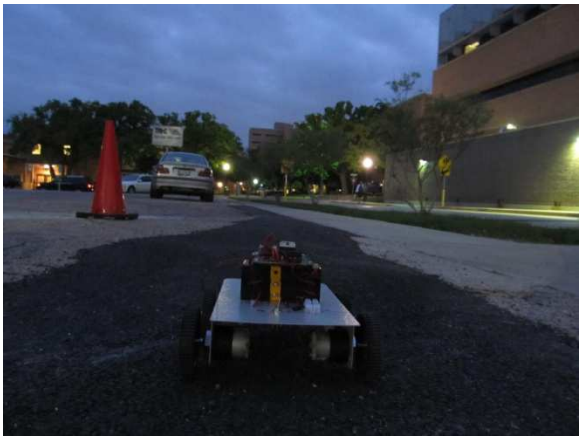

Figure 4-5 Test Run 2 - Relatively Smoother Asphalt surface

Figure 4-6 Test Run 2 - Relatively Rougher surface

The figure below illustrates the trend of the velocity slope variance values across the surface.

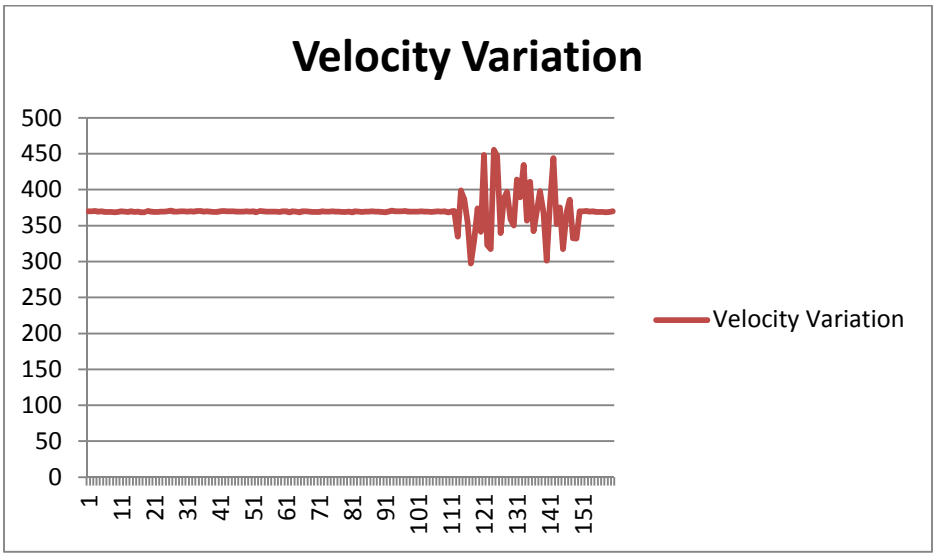

Figure 4-7 Test Run 2 - Velocity Variation with respect to distance

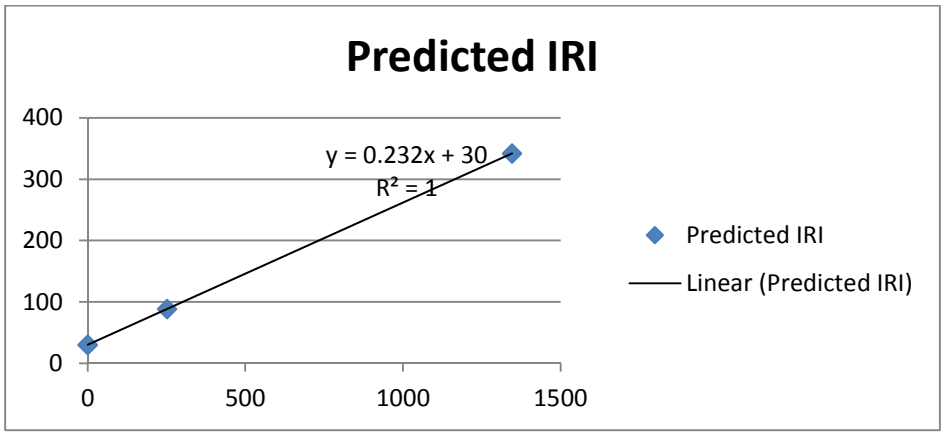

Figure 4-8 Test Run 2 - Predicted IRI

Table 4-2 Predicted IRI for Test Run-2

Distance	Velocity Variance Per 50 Ft	Predicted IRI(in/mi)	Total Variance	Total IRI(in/mi)
50	0.262914711	30.06099621	**429.8477359**	**132.6567307**
100	0.200488689	30.04651338		
150	252.376364	88.55131645		
200	1345.644919	342.1896212		

These IRI values were predicted once again using the equation $y = 0.2382x + 30.367$ with a Walker constant $k_{IRI} = 0.2382$ and constant $\varepsilon = 30.367$.

Clearly that we get low IRI prediction indicating smoother surface for the first 150 ft equivalent of data. That information matches with Figure 4-5. For the next ~70 ft of the surface we get high IRI predictions as is clear from Figure 4-6. This data was matched, bonafied and verified by our research advisor who has been a pioneer in the field of road profile measurement for over 40 years.

Chapter 5

CONCLUSIONS AND FUTURE WORK

5.1 Conclusions

From the results obtained in Chapter 4, we could successfully conclude that we could predict the IRI values for a given surface using the Walker constant and our data acquisition system within a reasonable range. This opens up the avenue to try this technique on several types of surfaces and obtain more predictions. Apart from the result itself, the implementation of the system was a success in itself.

In this research endeavor, we could successfully design and implement a low speed wirelessly controlled automated robot car which had a load bearing capability of ~2Kg and had 100 rpm motors on its wheels. The total cost of development of the robot was less than $50. Currently road profilers for asphalt measurement use a full-fledged vehicle mounted with all the sensors.

We also successfully used the Intel Galileo board mounted atop the system with an independent power supply using Lead Acid batteries. Our requirement was just 12 V of battery power. This made the data acquisition unit completely mobile and at very low power. Current systems use full-fledged generators inside the vehicles as they need to provide power to sophisticated sensors and data acquisition systems whereas our unit just required a low-power Intel Galileo board interfaced with ADXL345 accelerometer.

The implementation of such a portable and mobile unit, if implemented in field, would allow road contractors to readily and instantaneously obtain surface profile and IRI measurements as soon as asphalt is laid. Currently, they have to wait till the asphalt dries up and have to employ the above mentioned sophisticated profiling systems to obtain the same data.

Another feature that we could successfully implement is the ability to save the Data Acquisition information as files on the SD card mounted atop the Intel Galileo and retrieve them via the Ethernet. We even control the data acquisition start and stop from the laptop. This gives a potential user a lot of flexibility in terms of reducing redundancy and to eliminate start-stop speed variation conditions of the robot itself and obtain data at constant speed. That helps is getting much more stable readings and a better prediction.

5.2 Future work

Our work with this system went a long way and achieved what no other system for measurement of IRI had done. But there are still a few more improvements which future researchers can look into in order to make this system much more robust and probably industrial grade quality.

The biggest improvement is the ability to get actual IRI readings using a profiling system currently used by TXDOT. With our limited time and schedule, we could not get TXDOT employees to come here and do that for us. But future researchers in the same domain can plan that in their schedule and get actual data values. We have now relied on the acumen of our research advisor in order to validate the data we obtained, with TXDOT in the picture we could get more empirical evidence supporting this concept.

Future research endeavors can focus on having high precision industrial grade accelerometers with dedicated data acquisition systems in order to get more crisp and accurate predictions. We were limited by our schedule, the size of our robot, power supply constraints and also the procurement time for the said devices/sensors. With the sensors and system available to us we could get a good estimate of IRI, which leads me to believe that with more precise instruments it will only get better.

Another minor area of improvement that I can see is the addition of wireless capability to our system. In today's day and age, low-cost ready-to-use plug and play

wireless modules are available on the go, adding one to our system is the logical next step. Intel Galileo, in fact, does have on-board capability and the drivers in the kernel to support wireless devices.

With these above improvements, we believe we can make a full-fledged industrial grade data acquisition system, with practical use in the field of road profile measurement and IRI computation.

References

[1] R. Huang, I. Mao and H. Lee, '"Exploring the Deterioration Factors of RC Bridge Decks: A Rough Set Approach," Computer-Aided Civil and Infrastructure Engineering, vol. 25, no. 7, pp. 515-530.

[2] M.W. Sayers, S.M. Karamihas and The Regent of the University of Michigan, The little book of profiling Transportation Research Institute, 1998.

[3]A.P. Annan, "GPR for Infrastructure imaging",2003.

[4] http://www.dot.state.mn.us, "Introduction to International Roughness Index", 2007.

[5] http://www.vegarobokit.com/," L2 Wireless", 2010.

[6] https://learn.sparkfun.com/tutorials/galileo-getting-started-guide, "Galileo Getting started guide", 2013.

[7] http://wiki.androciti.com/,"I2C Arduino ADXL345",2010.

[8] https://www.sparkfun.com/tutorials/240, "ADXL345 Quickstart Guide", Jan 10, 2011.

Biographical Information

Joseph Mullassery Joemon Jose was born in Mumbai, India in 1984. He completed his undergraduate Electronics and Telecommunications engineering degree in 2006 from Mumbai University. He was an embedded firmware professional with lots of experience in the industry before pursuing MS in Electrical Engineering at The University of Texas at Arlington.

At the university his focus has been on transportation and instrumentation related research. This includes interfacing with various types of sensors, device driver development for RTOS/non-RTOS type platforms, low-level firmware and hardware development etc.